Int J Coal Sci Technol (2017) 4(1):50–59
DOI 10.1007/s40789-016-0148-8

Post-synthesis modification of porous organic polymers with amine: a task-specific microenvironment for CO_2 capture

Yankai Li[1] · Li Yang[1] · Xiang Zhu[1] · Jun Hu[1] · Honglai Liu[1]

Received: 25 January 2016 / Revised: 24 September 2016 / Accepted: 1 November 2016 / Published online: 28 November 2016

Abstract A porous organic polymer named FC-POP was facilely synthesized with extraordinary porosity and excellent stability. Further covalent incorporation of various amines including single amine group, multi-amine groups of diethylenediamine (DETA), and poly-amine groups of polyethylenimine (PEI) to the network gave rise to task-specific modification of the microenvironments to make them more suitable for CO_2 capture. As a result, significant boost of CO_2 adsorption capacity of 4.5 mmol/g (for FC-POP–CH_2DETA, 273 K, 1 bar) and the CO_2/N_2 selectivity of 736.1 (for FC-POP–CH_2PEI) were observed after the post-synthesis amine modifications. Furthermore, these materials can be regenerated in elevated temperature under vacuum without apparent loss of CO_2 adsorption capacity.

Keywords Porous organic polymers · Friedel–Crafts alkylation · Post-synthesis · Amine modification · CO_2 capture

1 Introduction

The rapidly increasing concentration of atmospheric carbon dioxide generated from combustion of fuels (include coal, petroleum and natural gas) has aroused environmental concern, as a result, carbon capture and sequestration (CCS) gradually gain their growing popularity (D'Alessandro et al. 2010; Sumida et al. 2011; Goeppert et al. 2012; Lu et al. 2013; Wang and Xu 2014; Romanov et al. 2015). Chemical absorption by aqueous solutions of ethanolamines (Brennecke and Gurkan 2010), which is most widely used CCS technique, suffer from several fatal defects including solvent loss, corrosion, and tremendous energy cost for the regeneration (Service 2004). So more efforts have been devoted to solid porous adsorbent. Various categories of novel materials with extraordinary porosity have been discovered, including silicas (Suhendi et al. 2013), zeolites (Wakihara et al. 2010), metal–organic frameworks (Li et al. 2014), zeolitic imidazolate frameworks (Cai et al. 2014) and carbon materials (Sevilla and Fuertes 2011). With the advantages of outstanding BET surface area and stability, tremendous porous organic polymers (POPs) have been designed (Jiang et al. 2009; Dawson et al. 2012; Zhao et al. 2012; Han et al. 2013; Liu et al. 2013; Zhu et al. 2013; Thompson et al. 2014; Zhu and Zhang 2014; Puthiaraj et al. 2015). More importantly, the organic skeletons of POPs give rise to their easy-to-functionalize nature so that enhancement of CO_2/N_2 selectivity is able to be realized via the incorporation of CO_2-philic groups into networks (Thomas 2010). Typically, PPNs (porous polymer networks) (Ben et al. 2009; Yuan et al. 2011) was synthesized with ultrahigh Brunner–Emmet–Teller (BET) surface area, the specific surface area of materials calculated by using adsorption theory developed by three scientists, namely Brunner, Emmet and Teller), some of which can be further incorporated by various groups, such as sulfonic acid, lithium sulfonate and ammonium sulfonate, to significantly improve the CO_2 uptake (3.6–3.7 mmol/g, 295 K, 1 bar) (Lu et al. 2011, 2013). However, in spite of their impressive performance, these polymers are difficult to be used for

✉ Jun Hu
junhu@ecust.edu.cn

[1] State Key Laboratory of Chemical Engineering, Department of Chemistry, East China University of Science and Technology, Shanghai 200237, China

industrial scale-up applications because of the harsh synthesis conditions.

Alternatively, a facile and efficient method has been reported, known as "knitting" aromatic building blocks to a polymeric skeleton. A large number of heterocyclic rings were picked as monomers to afford crosslinking networks by applying the new technique (Li et al. 2011; Woodward et al. 2014; Zhu et al. 2014; Xu et al. 2015). However, their modest CO_2 uptakes need great improvement for the future CO_2 capture applications (Luo et al. 2012).

Herein, a single-step procedure was adopted to facilely realize "knitting" strategy to afford a porous organic polymer via Friedel–Crafts alkylation (FC-POPs). Triptycene, which may allow for a high degree of internal free volume, was chosen as monomer, in order to deliver FC-POPs with abundant mesopores. The mesopores of FC-POPs shows a facility for further modifications, to investigate the influence of pore structure and nitrogen-site density on CO_2 adsorption. To realize this fancy, various groups with nitrogen-site including amine-group, diethylenediamine (DETA) and polyethylenimine (PEI) were grafted into the network to produce task-specific microenvironments by modifying microporosity and nitrogen-site density (Scheme. 1). Accordingly, the CO_2 adsorption capacity and selectivity of CO_2 over N_2 were significantly improved after the post-synthesis modifications.

2 Experiments

2.1 Materials and synthesis

Solvents, reagents and chemicals were purchased from Aldrich and TCI. All were used without any further purification.

2.1.1 Synthesis of FC-POP

Similar to Tan's method (Li et al. 2011), Triptycene (0.64 g, 2.5 mmol) and formaldehyde dimethyl acetal (1.14 g, 15.0 mmol) dissolving in 5 mL dichloroethane was added to a 25 mL flask. Anhydrous $FeCl_3$ (2.44 g, 15.0 mmol) was then added as a catalyst, and the mixture was stirred at 45 °C for 5 h and then heated to 80 °C for another 19 h. After cooling to room temperature, the mixture was filtered, washed by methanol for 3 times. The solid was collected, and extracted with methanol by Soxhlet apparatus for 24 h, brown solid was obtained after drying (yield ~95%).

2.1.2 Synthesis of FC-POP–CH_2Cl

A mixture of 0.30 g FC-POP, 1.50 g paraformaldehyde, 9.0 mL acetic acid, 4.5 mL phosphoric acid and 30.0 mL concentrated hydrochloric acid were charged in a flask, by

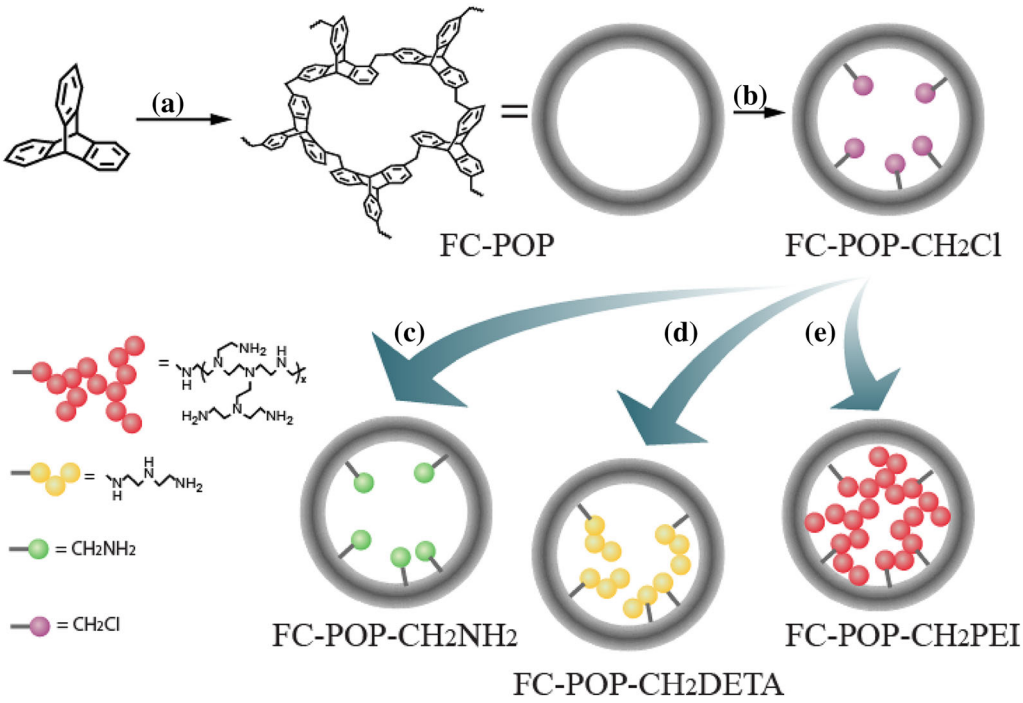

Scheme 1 Synthesis of FC-POP and its derivatives. The reaction conditions in each step; **a** formaldehyde dimethyl acetal, $FeCl_3$, dichloroethane, 45 °C, 5 h; 80 °C, 19 h; **b** paraformaldehyde, H_3PO_4, AcOH, HCl, 90 °C, 72 h; **c** i potassium phthalimide, DMF, 100 °C, 8 h; ii hydrazine monohydrate, EtOH, reflux, 20 h; **d** DETA, 90 °C, 72 h; **e** PEI, 90 °C, 72 h

following a well-known method (Lu et al. 2012). The flask was sealed, then the mixture was heated to 90 °C and maintained for 3 days. After cooling to room temperature, the solid was collected and washed with water and methanol for three times, then dried to afford FC-POP–CH_2Cl.

2.1.3 Synthesis of FC-POP–CH_2NH_2

A mixture of FC-POP–CH_2Cl (0.20 g), potassium phthalimide (1.19 g) and 20.0 mL *N*,*N*-dimethylformamide (DMF) was stirred at 100 °C for 8 h under an argon atmosphere, similar to a well-known method (Ilhan et al. 1999). The cooled mixture was filtered and cursorily washed by DMF. The resulting phthalimide derivative was mixed with 1 mL of hydrazine monohydrate in 12 mL ethanol. The reaction was refluxed for 20 h. The reaction mixture was filtered and washed subsequently by DMF, water and MeOH, then dried to afford FC-POP–CH_2NH_2.

2.1.4 Synthesis of FC-POP–CH_2DETA

A mixture of 0.10 g FC-POP–CH_2Cl and 10.0 mL diethylenetriamine (DETA) was charged in a flask, according to a well-known method (Lu et al. 2012). The flask was sealed then heated to 90 °C and maintained for 3 days. After cooling to room temperature, the solid was collected and washed with water and methanol for several times, then dried to afford FC-POP–CH_2DETA.

2.1.5 Synthesis of FC-POP–CH_2PEI

In a fashion similar to the synthesis of FC-POP–CH_2DETA, 0.10 g FC-POP–CH_2Cl and 10.0 g polyethylene imine (PEI, mw = 600) was reacted to afford FC-POP–CH_2PEI.

2.2 Characteristics

Thermogravimetry analysis (TGA) were performed under N_2 on a NETZSCH STA449F3, with a heating rate of 10 °C /min. ^{13}C NMR measurements were performed on a 9.4 T Bruker Avance spectrometer at a Larmor frequency of 100.6 MHz. Measurements were made with a 4 mm MAS probe spinning at 15 kHz. Chemical shifts were externally referenced to TMS ($\delta = 0$ ppm) using the methyl resonance of hexamethylbenzene (17.5 ppm relative to TMS). Nitrogen adsorption isotherms were measured at 77 K using Micromeritics ASAP 2020 static volumetric analyzer. Before adsorption measurements the polymer was degassed at 110 °C under vacuum. The BET surface area was calculated within the relative pressure range 0.05–0.30. Total volume was calculated at $p/p_0 = 0.98$ and micropore volume was calculated by t-plot method. FTIR data were obtained using a Nicolet Magna-IR 550 spectrometer. Elemental analysis was determined using a Vario EL III Elemental Analyzer (Elementar, Germany).

2.3 Gas adsorption experiments

2.3.1 Gas adsorption and desorption isotherms

Both of gas adsorption and desorption isotherms of POPs were measured using a Micromeritics ASAP 2020 static volumetric analyzer at the setting temperature. Prior to each adsorption experiment, the samples were degassed for 12 h at 110 °C ensuring that the residual pressure fell below 0.2 Pa and then cooled down to the target temperatures, followed by introduction of a single component gas (CO_2 or N_2) into the system. Once the adsorption process finished, the desorption experiment was automatically initiated. In the desorption stage, gas pressure gradually decreased and the corresponding amount of residue adsorbed gas was measured and calculated by the instrument.

2.3.2 Fits of isotherms

For FC-POP and FC-POP–CH_2Cl, single-site Langmuir fit is appropriate. Their isotherms can be described by the Eq. (1).

$$q = q_{\text{sat}} \frac{bp}{1 + bp} \tag{1}$$

where, b is a parameter in the pure component Langmuir isotherm (Pa^{-1}), p represents gas pressure (Pa), q is molar loading of gas components (mol/kg) and q_{sat} is saturation capacity of gas components (mol/kg).

For FC-POP–CH_2NH_2, FC-POP–CH_2DETA and FC-POP–CH_2PEI, both physical and chemical interaction should be taken into account so that dual-site Langmuir (Eq. 2) fitting is fine.

$$q = q_{\text{sat},1} \frac{b_1 p}{1 + b_1 p} + q_{\text{sat},2} \frac{b_2 p}{1 + b_2 p} \tag{2}$$

where two distinct adsorption sites are assumed to be existed, so there are four parameters in the equation, namely $q_{\text{sat},1}$, b_1, $q_{\text{sat},2}$ and b_2.

2.3.3 Adsorption enthalpy

For CO_2 adsorption, fits of isotherms were used to calculate adsorption enthalpy by employing Clausius–Clapeyron equation (Eq. 3).

$$\ln\left(\frac{p_1}{p_2}\right) = \Delta H\left(\frac{1}{T_1} - \frac{1}{T_2}\right) \tag{3}$$

where p_i is the pressure for isotherm i, T_i is the temperature for isotherm i, R is 8.315 J/(K mol).

2.3.4 IAST calculation

Pure-component isotherm fitting parameters were used for calculating ideal adsorbed solution theory (IAST) binary-gas adsorption selectivity (Myers and Prausnitz 1965), defined as the Eq. (4):

$$S = \frac{q_1/q_2}{p_1/p_2} \tag{4}$$

where p_i represents partial pressure of gas i and q_i is the corresponding pure-component gas uptake amount at p_i. The IAST calculations were carried out for flue gas model (binary mixture containing 15% CO_2 and 85% N_2).

3 Results and discussions

3.1 General characteristics

FC-POP was synthesized in good yield via a simple Friedel–Crafts reaction. Triptycene was selected to be the monomer because of its rigid molecular structure, which would lead to a microporous skeleton with the extraordinary porosity and high stability. The resulting FC-POP was found to be insoluble in common organic solvents, such as water, methanol, dichloromethane, tetrahydrofuran, acetone and hexane. The chemical structure of FC-POP was confirmed by ^{13}C cross-polarization magic-angle spinning (CP/MAS) NMR (Fig. 1). In the NMR spectrum, the resonance peaks at 139 and 130 ppm correspond to the substituted aromatic carbons of triptycene, while the resonance peak at 120 correspond to their non-substitute counterparts. Resonance peaks at 46–50 belong to the bridgehead carbons of triptycene. The peaks around 32 ppm ascribes to the carbons of methylene linkers. Besides, high thermostability of FC-POP was proved by thermogravimetric analysis (TGA) that little apparent weight loss below 350 °C (Fig. 2a).

In order to modify the microenvironment, FC-POP was covalently incorporated by various moieties to obtain a series of amine-functionalized FC-POPs (Scheme 1). FC-POP–CH_2Cl, which containing vivacious chloromethyl groups, was first been prepared as an intermediate and chloromethyl groups were then substituted by various amines to afford FC-POP–CH_2NH_2, FC-POP–CH_2DETA and FC-POP–CH_2PEI. The peaks at 75–93 ppm in the solid-state NMR spectrum of FC-POP–CH_2Cl suggested the graft of chloromethyl to the polymeric skeleton (Fig. 1). The appearance of peaks around 200 ppm for the

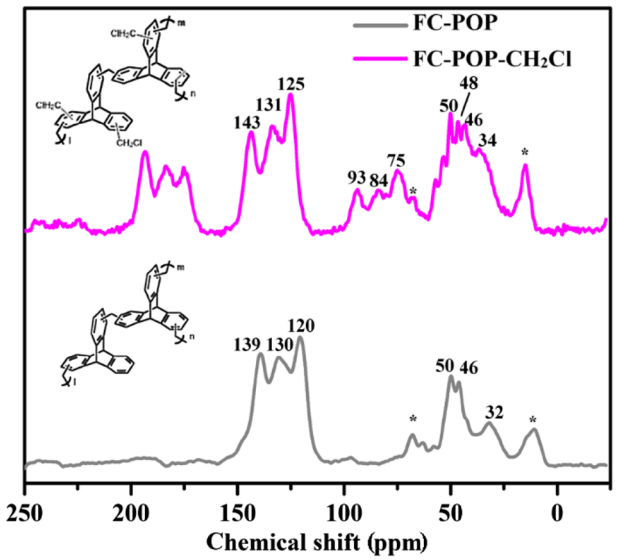

Fig. 1 Solid State ^{13}C cross-polarization magic-angle spinning (CP/MAS) NMR of FC-POP and FC-POP–CH_2Cl

spectrum of FC-POP–CH_2Cl ascribed to the carbonyl group of residual acetic acid and paraformaldehyde that involved in the synthesis. Successful incorporation of functional amine groups were confirmed by Fourier Transform infrared spectroscopy (FTIR) that prosperous graft of amine groups can be proved by enhancement of the band around 1650 cm^{-1} (Fig. 2b). The amine-modified POPs also exhibit quite good thermal stability according to the thermogravimetric analysis results (Fig. 2a).

To quantitatively describe the density of functional groups, element analysis was conducted for the polymers. The calculated density of nitrogen element (mmol/g) shows a significant growth of nitrogen density in sequence of FC-POP–CH_2NH_2 (3.46 mmol/g), FC-POP–CH_2DETA (8.43 mmol/g) and FC-POP–CH_2PEI (11.47 mmol/g) (Table 1). Therefore, the tailor-made functional group would make the nitrogen-site density controllable in the microenvironment of these POPs.

Porosity of these materials was measured by nitrogen adsorption at 77 K (Fig. 3a) and the surface areas were calculated by the BET model. FC-POP exhibits extraordinary porosity, with the BET surface area as high as 1540 m^2/g. The adsorption/desorption isotherms for FC-POP is not closed, mainly because of a swelling of polymer matrix at 77 K (Zhang et al. 2012). After the incorporation of functional groups, the BET surface area dropped correspondingly. The S_{BET} data drops to 939 m^2/g for FC-POP–CH_2NH_2, 636 m^2/g for FC-POP–CH_2DETA and only 129 m^2/g for FC-POP–CH_2PEI. For the adsorption isotherms of these FC-POPs, swift climb at low pressure ($p/p_0 < 0.001$) is contributed by micropores of these FC-POPs, while hysteresis at higher pressure proves the

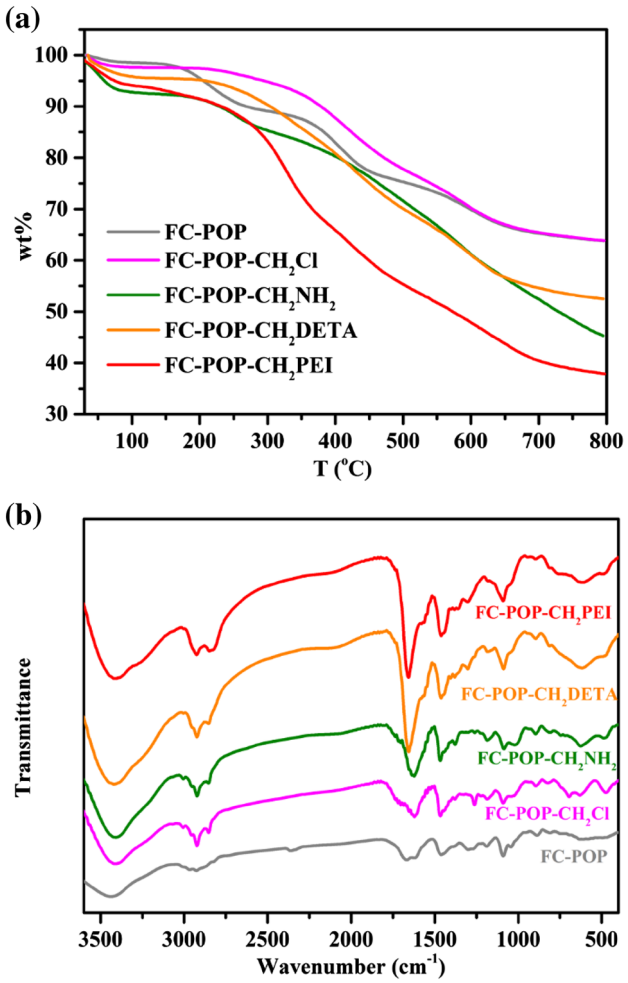

Fig. 2 Thermogravimetric analysis (TGA) (**a**) and Fourier Transform infrared spectroscopy (FTIR) (**b**) of FC-POP, FC-POP–CH_2Cl, FC-POP–CH_2NH_2, FC-POP–CH_2DETA and FC-POP–CH_2PEI

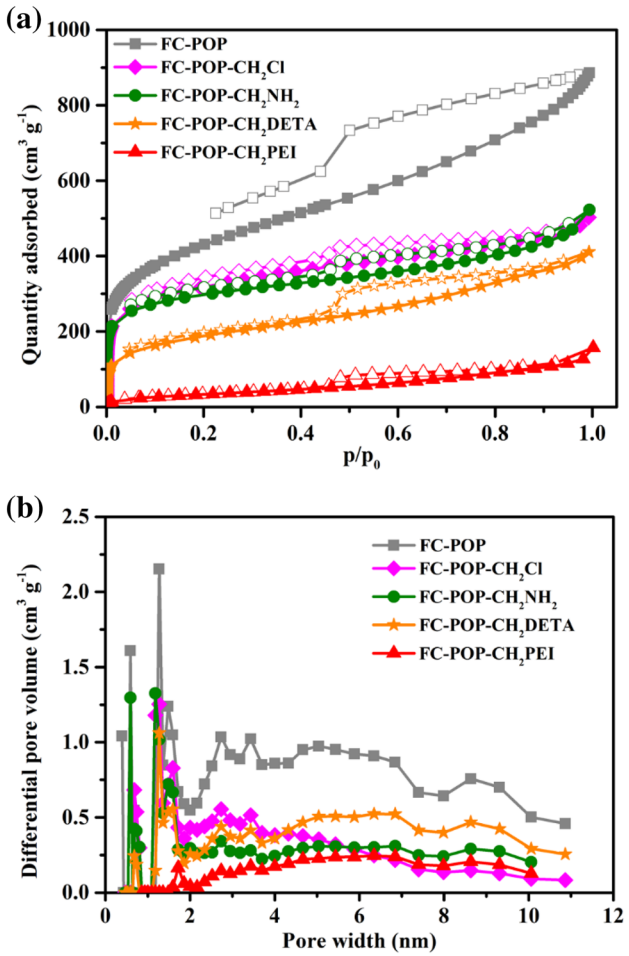

Fig. 3 **a** Nitrogen adsorption isotherms at 77 K, *solid symbols* for adsorption curves and *hollow symbols* for desorption ones; **b** pore size distribution calculated by NLDFT method

existence of mesopores. Pore size distribution caculated by non-local density functional theory (NLDFT) method also confirmed the presence of both micropores and mesopores (Fig. 3b). The mesopores, facilitating the mass transfer during the gas uptake process, can act as the transport channels (Liao et al. 2014). On the other hand, micropores, enhancing the interaction between the wall and CO_2 molecules, can act as the adsorption active points (Islamoglu et al. 2013). As a result, both of them are crucial to CO_2 adsorption applications. For FC-POP, V_{micro}/V_{total} value (the ratio of micropore volume to the total pore volume) is as low as 0.0842, demonstrating the existance of impressive mesopores. After grafting amines into the network, the microenvironment of pore structure has altered. For example, V_{micro} value of FC-POP–CH_2NH_2 (0.251 cm^3/g) doubles that of FC-POP (0.113 cm^3/g), and its V_{micro}/V_{total} value upsurges to 0.311. Accordingly, the

Table 1 Elemental analysis and calculated N-site density for FC-POP, FC-POP–CH_2Cl, FC-POP–CH_2NH_2, FC-POP–CH_2DETA and FC-POP–CH_2PEI

POPs	N (%)	C (%)	H (%)	N-site density (mmol N/g)
FC-POP	~0	77.78	4.89	~0
FC-POP–CH_2Cl	~0	71.60	5.34	~0
FC-POP–CH_2NH_2	4.10	73.93	6.56	3.46
FC-POP–CH_2DETA	10.79	73.21	7.47	8.43
FC-POP–CH_2PEI	14.53	67.90	8.04	11.47

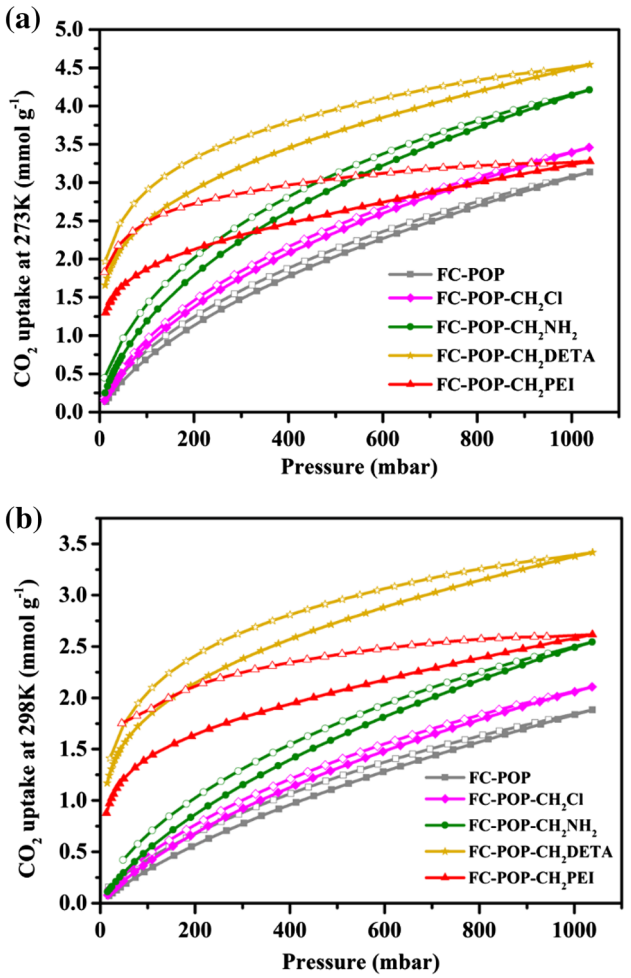

Fig. 4 CO_2 adsorption isotherms measured at 273 K (**a**) and 298 K (**b**), *solid symbols* for adsorption curves and *hollow symbols* for desorption ones

incorporation of functional groups may spatially separate mesopores into several micropores, result in the modified microenvironment of these FC-POPs through the redistribution of pore volumes, making the resulting POPs more suitable for CO_2 capture applications.

3.2 CO_2 adsorption performance

Excellent porosity and affluent nitrogen density are beneficial to boost CO_2 adsorption capacity for these amine-modified POPs. Indeed, significant growth of CO_2 uptake was observed after amine-grafting (Fig. 4). For FC-POP–CH_2NH_2 and FC-POP–CH_2DETA, under the pressure of 1 bar, CO_2 adsorption capacity reaches 4.2/2.5 and 4.5/3.4 mmol/g at 273/298 K, much higher than that of pristine FC-POP (3.1/1.8 mmol/g at 273/298 K). Notably, FC-POP–CH_2PEI also exhibits impressive CO_2 storage ability (3.2/2.6 mmol/g at 273/298 K) in spite of its poor BET surface area. There are two dominant contributions for CO_2 adsorption capacity, the chemical adsorption contributed by amine groups (denoted as the nitrogen-site density) and the physical adsorption contributed by porosity (denoted as the BET surface area). For these FC-POPs with diverse incorporated amines, the hysteresis loops between their adsorption/desorption isotherms could be clear evidences of chemical interactions between amine groups and CO_2 molecules. However, in our work, the growth of the nitrogen site density can significantly increase the CO_2 adsorption enthalpy but decrease the BET surface area (Table 2). FC-POP–CH_2DETA exhibited the excellent CO_2 adsorption enthalpy (54.0 kJ/mol) yet maintained considerable BET surface area (636 m^2/g). That means, FC-POP–CH_2DETA reached a compromise between these two factors, hence its high CO_2 adsorption capacity.

To further understand the influence of various functional groups on adsorption behavior, CO_2 adsorption enthalpies were calculated by the dual-site Langmuir fitting of CO_2 adsorption isotherms at 273 and 298 K based on Clausius–Claperyron equation. Figure 5a illustrates a plot of the CO_2 adsorption enthalpies as a function of loading. It is obvious

Table 2 Characteristics of POPs in this work

POPs	N-site density[a] (mmol N/g)	S_{BET} (m^2/g)	V_{total} (cm^3/g)[b]	CO_2 uptake[c] (mmol/g) (273 K/298 K)	Q_{st}^d (kJ/mol)	Selectivity[e] (298 K)
FC-POP	~0	1540	1.330	3.1/1.8	26.4	12.62
FC-POP–$CHCl_2$	~0	1058	0.801	3.4/2.1	27.9	19.32
FC-POP–CH_2NH_2	3.46	939	0.808	4.2/2.5	37.9	31.58
FC-POP–CH_2DETA	8.43	636	0.636	4.5/3.4	54.0	167.8
FC-POP–CH_2PEI	11.47	129	0.243	3.2/2.6	59.6	736.1

[a] Values were calculated from elemental analysis

[b] Total volumes calculated at $p/p_0 = 0.98$

[c] Measured at the pressure of 1 bar

[d] Calculated CO_2 enthalpy of adsorption by applying Clausius–Claperyon equation

[e] IAST selectivity (1 bar) for CO_2/N_2 calculated from pure component fits under flue gas model (CO_2/N_2 = 15:85)

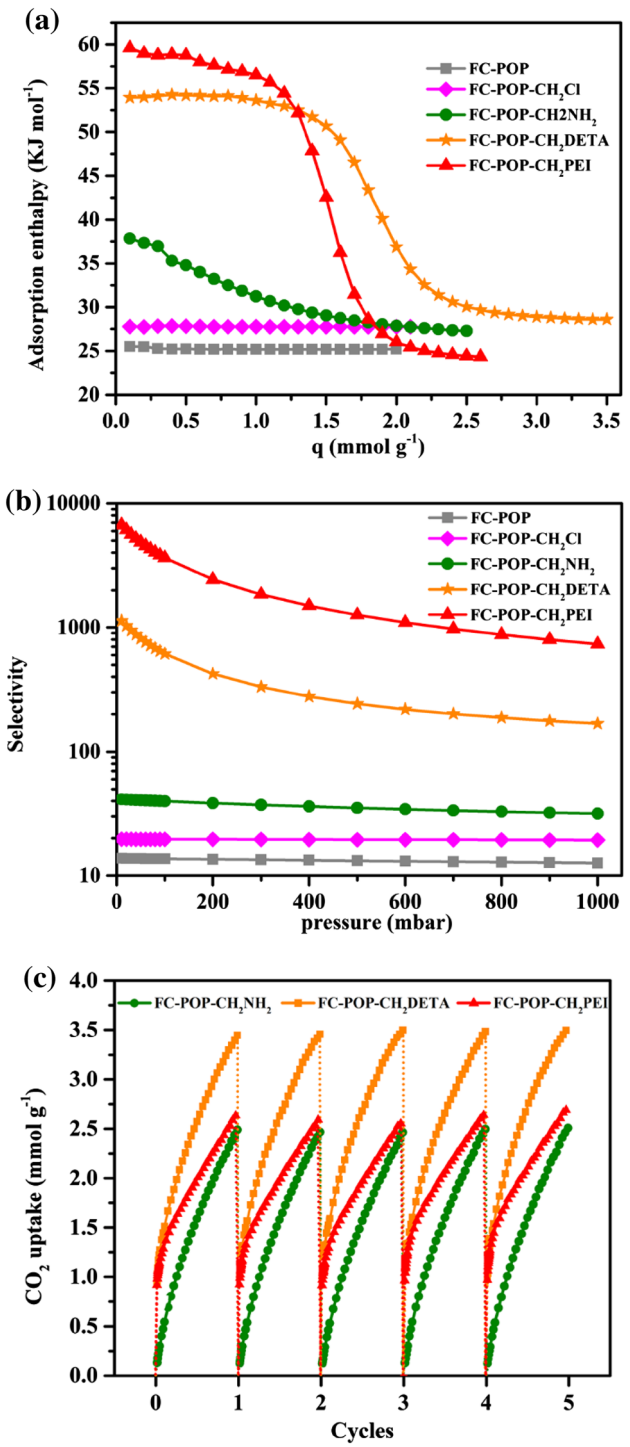

Fig. 5 **a** CO_2 adsorption enthalpy for POPs; **b** The selectivity of POPs for CO_2 over N_2 isotherms obtained from IAST calculations; **c** Cyclic CO_2 adsorption for POPs on an ASAP 2020

that FC-POP–CH_2NH_2, FC-POP–CH_2DETA and For FC-POP–CH_2PEI exhibit dramatically high CO_2 adsorption enthalpy values as 37.9, 54.0 and 59.6 kJ/mol at low loadings, respectively; much higher than that of FC-POP (26.4 kJ/mol). The high adsorption enthalpy values ascribe to strong interactions between amine-functional groups in FC-POPs and CO_2 molecules, for the presence of amines gives rise to chemical adsorption towards CO_2. It is worth mentioned that the adsorption enthalpy value of FC-POP–CH_2DETA remains a high value even when the CO_2 loading reaches 1.5 mmol/g, suggesting its abundant chemical adsorption sites, hence the extraordinary CO_2 adsorption capacity. The adsorption enthalpy values of amine-functionalized POPs show a similar sequence of nitrogen content, so that the nitrogen-site density are the dominant contribution for the strong affinity to CO_2 in the microenvironment of these FC-POPs.

The excellent CO_2 uptake performance and outstanding adsorptive affinity of these FC-POPs ensure their adsorption selectivity. The ideal adsorption solution theory (IAST) proposed by Myers and Prausnitz (1965) was used to calculate the adsorption selectivity of CO_2/N_2 for these materials. Fits of pure component isotherms were plotted to determine the molar uptakes at specified partial pressures in the bulk gas mixture and the selectivity was calculated under the simulated flue gas model ($CO_2/N_2 = 15/85$). The results suggested that the presence of incorporated amines in FC-POPs prompts the CO_2/N_2 selectivity (Fig. 5b). The selectivity value of FC-POP–CH_2NH_2 (31.58) is about 2.5 times higher than that of FC-POP (12.62) at 298 K. Significantly, the CO_2/N_2 selectivity value of FC-POP–CH_2DETA and FC-POP–CH_2PEI soar to 167.8 and 736.1 (298 K), respectively, thanks to their advantageous microenvironment including the microporosity and outstanding nitrogen-site density within the pores. For FC-POP–CH_2PEI, although CO_2 uptake seems modest comparing to the reported values [MCTP-1 (Puthiaraj et al. 2015), 2.7 mmol/g, 298 K, BILP-4 (Rabbani and El-Kaderi 2012), 3.59 mmol/g, 298 K; FCTF-1-600 (Zhao et al. 2013), 3.41 mmol/g, 273 K], the selectivity value is comparable to many other excellent reported POPs [azo-COP-2 (Patel et al. 2013), 130.6, 298 K; Py-1 (Luo et al. 2012), 117, 273 K; PPN-6-CH_2DETA (Lu et al. 2012), 442, 295 K] (Table 3). The excellent selectivity of FC-POP–CH_2PEI ascribe to the strong adsorption enthalpy towards CO_2 (59.6 kJ/mol). Furthermore, the introduction of PEI moieties can effectively enhance the selectivity, because flexible PEI can block the pores of POPs to interfere the N_2 adsorption while CO_2 can infiltrate into the void of PEI chains and even swell the pores due to its high polarizability and quadrupole moment (Sung and Suh 2014). Although recently reported PEI (40 wt%) ⊂ PAF-5 (Sung and Suh 2014) exhibited even higher selectivity (1200, 298 K) than FC-POP–CH_2PEI, the latter still stands out in regards to the physicochemical stability arising from covalent bonding amine to the network. Overall, the selectivity value relies on pore structure and CO_2 adsorption enthalpies of polymers, so the adjustment of task-

Table 3 Summary of surface area, CO_2 uptake, selectivity and adsorption enthalpy (Qst) in selected POPs (with excellent reported results)

POPs	S_{BET} (m^2/g)	T (K)	CO_2 uptake (mmol/g)	IAST selectivity	Q_{st} (kJ/mol)	Ref.
FC-POP–CH_2NH_2	939	298	2.5	31.6	37.9	This work
		273	4.2	40.9		
FC-POP–CH_2DETA	636	298	3.4	167.8	54.0	This work
		273	4.5	194.3		
FC-POP–CH_2PEI	129	298	2.6	736.1	64.0	This work
		273	3.2	720.8		
TB-MOP	913	298	2.6	25	30.2	(Zhu et al. 2014)
		273	4.1	46		
FCTF-1-600	1535	298	3.41	19	30	(Zhao et al. 2013)
		273	5.53			
CMP-1-$(OH)_2$	1043	298	1.07		27.6	(Dawson et al. 2011)
		273	1.80			
BILP-4	1135	298	3.59	32[a]	28.7	(Rabbani and El-Kaderi 2012)
		273	5.34	79[a]		
PECONF-3	851	298	2.47	22	26	(Mohanty et al. 2011)
		273	3.49	60		
azo-COP-2	729	298	1.53	130.6	24.8	(Patel et al. 2013)
		273	2.56	109.6		
CPOP	2220	273	4.82	25[b]	27	(Chen et al. 2012)
Py-1	437	273	2.7	117[a]	36	(Luo et al. 2012)
ALP-1	1235	273	5.37	40	29.2	(Arab et al. 2014)
		298	3.25	28		
HBC-POP-1	688	298	1.2			(Thompson et al. 2014)
		273	2.1			
PPN-6-SO_3H	1254	295	3.6	150	30.4	(Lu et al. 2011)
PPN-6-SO_3Li	1186	295	3.7	414	35.7	(Lu et al. 2011)
PPN-6-CH_2DETA	555	295	4.3	442	56	(Lu et al. 2012)
PEI(40 wt%) ⊂ PAF-5	40.3	298	2.5	1200[c]	68.7	(Sung and Suh 2014)
MCTP-1	1452	298	2.7	15.4[a]	40.0	(Puthiaraj et al. 2015)
		273	4.6			

specific microenvironment would be an effective approach to improve CO_2/N_2 selectivity.

To test the regeneration of the FC-POPs, cycling experiments were conducted on an ASAP 2020 analyzer (Fig. 5c). For each cycle, the adsorbents were saturated with CO_2 up to 1 bar at 298 K followed by a high vacuum (0.2 Pa) at 80 °C for 90 min. The CO_2 adsorption capacity in each cycle almost reached the same point, with no apparent loss of uptake amount in the cycling test.

4 Conclusions

A highly porous FC-POP, which was facilely synthesized via Freidel–Crafts reaction, was incorporated by various amines to afford FC-POP–CH_2NH_2, FC-POP–CH_2DETA and FC-POP–CH_2PEI. Both microporosity and excellent amine-affinity towards CO_2 ensured those amine-functionalized polymers extraordinary CO_2 selective adsorption performance. The CO_2 adsorption capacity reached as high as 4.5 mmol/g at 273 K and 3.4 mmol/g at 298 K (1 bar) for FC-POP–CH_2DETA; and the CO_2/N_2 selectivity soared to 736.1 at 298 K (1 bar) for FC-POP–CH_2PEI. The reason is, that the incorporation of task-specific functional groups would work as a dual regulations for the microenviroment of POPs. The dual regulations, namely the modifications of pore structure as well as the basic amine density, improved microporosity and adsorption enthalpy of CO_2 apparently and further enhanced the CO_2 capture performance.

Acknowledgements Financial supports for this study are provided by the National Key Technology Support Program of China (2013CB733501), the National Natural Science Foundation of China (Nos. 91334203, 21676080), the project of FP7-PEOPLE-2013-IRSES (PIRSES-GA-2013-612230).

Compliance with ethical standards

Conflict of interest The authors declare no competing financial interests.

References

Arab P, Rabbani MG, Sekizkardes AK, İslamoğlu T, El-Kaderi HM (2014) Copper(I)-catalyzed synthesis of nanoporous azo-linked polymers: impact of textural properties on gas storage and selective carbon dioxide capture. Chem Mater 26:1385–1392. doi:10.1021/cm403161e

Ben T et al (2009) Targeted synthesis of a porous aromatic framework with high stability and exceptionally high surface area. Angew Chem Int Ed 48:9457–9460. doi:10.1002/anie.200904637

Brennecke JF, Gurkan BE (2010) Ionic liquids for CO_2 capture and emission reduction. J Phys Chem Lett 1:3459–3464. doi:10.1021/jz1014828

Cai W et al (2014) Thermal structural transitions and carbon dioxide adsorption properties of zeolitic imidazolate framework-7 (ZIF-7). J Am Chem Soc 136:7961–7971. doi:10.1021/ja5016298

Chen Q et al (2012) Microporous polycarbazole with high specific surface area for gas storage and separation. J Am Chem Soc 134:6084–6087. doi:10.1021/ja300438w

D'Alessandro DM, Smit B, Long JR (2010) Carbon dioxide capture: prospects for new materials. Angew Chem Int Ed 49:6058–6082. doi:10.1002/anie.201000431

Dawson R, Adams DJ, Cooper AI (2011) Chemical tuning of CO_2 sorption in robust nanoporous organic polymers. Chem Sci 2:1173–1177. doi:10.1039/C1SC00100K

Dawson R, Stevens LA, Drage TC, Snape CE, Smith MW, Adams DJ, Cooper AI (2012) Impact of water coadsorption for carbon dioxide capture in microporous polymer sorbents. J Am Chem Soc 134:10741–10744. doi:10.1021/ja301926h

Goeppert A, Czaun M, Surya Prakash GK, Olah GA (2012) Air as the renewable carbon source of the future: an overview of CO_2 capture from the atmosphere. Energy Environ Sci 5:7833–7853. doi:10.1039/C2EE21586A

Han Y, Zhang L-M, Zhao Y-C, Wang T, Han B-H (2013) Microporous organic polymers with ketal linkages: synthesis characterization, and gas sorption properties. ACS Appl Mater Interfaces 5:4166–4172. doi:10.1021/am400251h

Ilhan F, Gray M, Blanchette K, Rotello VM (1999) Control of polymer solution structure via intra- and intermolecular aromatic stacking. Macromolecules 32:6159–6162. doi:10.1021/ma990724z

Jiang J-X et al (2009) Microporous poly(tri(4-ethynylphenyl)amine) networks: synthesis, properties, and atomistic simulation. Macromolecules 42:2658–2666. doi:10.1021/ma802625d

Li B et al (2011) A new strategy to microporous polymers: knitting rigid aromatic building blocks by external cross-linker. Macromolecules 44:2410–2414. doi:10.1021/ma200630s

Li L et al (2014) A crystalline porous coordination polymer decorated with nitroxyl radicals catalyzes aerobic oxidation of alcohols. J Am Chem Soc 136:7543–7546. doi:10.1021/ja5019095

Liao Y, Weber J, Faul CFJ (2014) Conjugated microporous polytriphenylamine networks. Chem Commun 50:8002–8005. doi:10.1039/C4CC03026E

Liu D-P, Chen Q, Zhao Y-C, Zhang L-M, Qi A-D, Han B-H (2013) Fluorinated porous organic polymers via direct C-H arylation polycondensation. ACS Macro Lett 2:522–526. doi:10.1021/mz4001699

Lu W, Yuan D, Sculley J, Zhao D, Krishna R, Zhou H-C (2011) Sulfonate-grafted porous polymer networks for preferential CO_2 adsorption at low pressure. J Am Chem Soc 133:18126–18129. doi:10.1021/ja2087773

Lu W, Sculley JP, Yuan D, Krishna R, Wei Z, Zhou H-C (2012) Polyamine-tethered porous polymer networks for carbon dioxide capture from flue gas. Angew Chem Int Ed 51:7480–7484. doi:10.1002/anie.201202176

Lu W, Verdegaal WM, Yu J, Balbuena PB, Jeong H-K, Zhou H-C (2013) Building multiple adsorption sites in porous polymer networks for carbon capture applications Energy. Environ Sci 6:3559–3564. doi:10.1039/C3EE42226G

Luo Y, Li B, Wang W, Wu K, Tan B (2012) Hypercrosslinked aromatic heterocyclic microporous polymers: a new class of highly selective CO_2 capturing materials. Adv Mater 24:5703–5707. doi:10.1002/adma.201202447

Mohanty P, Kull LD, Landskron K (2011) Porous covalent electron-rich organonitridic frameworks as highly selective sorbents for methane and carbon dioxide. Nat Commun 2:401

Myers AL, Prausnitz JM (1965) Thermodynamics of mixed-gas adsorption. AlChE J 11:121–127. doi:10.1002/aic.690110125

Patel HA, Hyun Je S, Park J, Chen DP, Jung Y, Yavuz CT, Coskun A (2013) Unprecedented high-temperature CO_2 selectivity in N_2-phobic nanoporous covalent organic polymers. Nat Commun 4:1357

Puthiaraj P, Cho S-M, Lee Y-R, Ahn W-S (2015) Microporous covalent triazine polymers: efficient Friedel-Crafts synthesis and adsorption/storage of CO_2 and CH_4. J Mater Chem A 3:6792–6797. doi:10.1039/C5TA00665A

Rabbani MG, El-Kaderi HM (2012) Synthesis and characterization of porous benzimidazole-linked polymers and their performance in small gas storage and selective uptake. Chem Mater 24:1511–1517. doi:10.1021/cm300407h

Romanov V, Graeser L, Jikich S, Soong Y, Irdi G (2015) Coal–gas interaction: implications of changes in texture and porosity. Int J Coal Sci Technol. doi:10.1007/s40789-015-0098-6

Service RF (2004) Choosing a CO_2 separation technology. Science 305:963. doi:10.1126/science.305.5686.963

Sevilla M, Fuertes AB (2011) Sustainable porous carbons with a superior performance for CO_2 capture Energy. Environ Sci 4:1765–1771. doi:10.1039/C0EE00784F

Suhendi A, Nandiyanto ABD, Munir MM, Ogi T, Gradon L, Okuyama K (2013) Self-assembly of colloidal nanoparticles inside charged droplets during spray-drying in the fabrication of nanostructured particles. Langmuir 29:13152–13161. doi:10.1021/la403127e

Sumida K et al (2011) Carbon dioxide capture in metal-organic frameworks. Chem Rev 112:724–781. doi:10.1021/cr2003272

Sung S, Suh MP (2014) Highly efficient carbon dioxide capture with a porous organic polymer impregnated with polyethylenimine. J Mater Chem A 2:13245–13249. doi:10.1039/C4TA02861A

Thomas A (2010) Functional materials: from hard to soft porous frameworks. Angew Chem Int Ed 49:8328–8344. doi:10.1002/anie.201000167

Thompson CM, Li F, Smaldone RA (2014) Synthesis and sorption properties of hexa-(peri)-hexabenzocoronene-based porous organic polymers. Chem Commun 50:6171–6173. doi:10.1039/C4CC02213K

Wakihara T, Sato K, Inagaki S, Tatami J, Komeya K, Meguro T, Kubota Y (2010) Fabrication of fine zeolite with improved catalytic properties by bead milling and alkali treatment. ACS Appl Mater Interfaces 2:2715–2718. doi:10.1021/am100642w

Wang J, Xu S (2014) CO_2 capture RD&D proceedings in China Huaneng Group. Int J Coal Sci Technol 1:129–134. doi:10.1007/s40789-014-0013-6

Woodward RT et al (2014) Swellable, water- and acid-tolerant polymer sponges for chemoselective carbon dioxide capture. J Am Chem Soc 136:9028–9035. doi:10.1021/ja5031968

Xu S, Song K, Li T, Tan B (2015) Palladium catalyst coordinated in knitting N-heterocyclic carbene porous polymers for efficient Suzuki-Miyaura coupling reactions. J Mater Chem A 3:1272–1278. doi:10.1039/C4TA05265J

Yuan D, Lu W, Zhao D, Zhou H-C (2011) Highly stable porous polymer networks with exceptionally high gas-uptake capacities. Adv Mater 23:3723–3725. doi:10.1002/adma.201101759

Zhang C, Liu Y, Li B, Tan B, Chen C-F, Xu H-B, Yang X-L (2012) Triptycene-based microporous polymers: synthesis and their gas storage properties. ACS Macro Lett 1:190–193. doi:10.1021/mz200076c

Zhao Y-C, Wang T, Zhang L-M, Cui Y, Han B-H (2012) Facile approach to preparing microporous organic polymers through benzoin condensation. ACS Appl Mater Interfaces 4:6975–6981. doi:10.1021/am302163p

Zhao Y, Yao KX, Teng B, Zhang T, Han Y (2013) A perfluorinated covalent triazine-based framework for highly selective and water-tolerant CO_2 capture. Energy Environ Sci 6:3684–3692. doi:10.1039/C3EE42548G

Zhu Y, Zhang W (2014) Reversible tuning of pore size and CO_2 adsorption in azobenzene functionalized porous organic polymers. Chem Sci 5:4957–4961. doi:10.1039/C4SC02305F

Zhu X et al (2013) Efficient CO_2 capture by a 3D porous polymer derived from Tröger's base. ACS Macro Lett 2:660–663. doi:10.1021/mz4003485

Zhu X et al (2014) Efficient CO_2 capture by a task-specific porous organic polymer bifunctionalized with carbazole and triazine groups. Chem Commun 50:7933–7936. doi:10.1039/C4CC01588F